CrossMark

Ethanol Exacerbates Manganese-Induced Neurobehavioral Deficits, Striatal Oxidative Stress, and Apoptosis Via Regulation of p53, Caspase-3, and Bax/Bcl-2 Ratio-Dependent Pathway

Kpobari W. Nkpaa[1] · Ifeoluwa O. Awogbindin[2] · Benjamin A. Amadi[1] · Amos O. Abolaji[2] · Isaac A. Adedara[2] · Matthew O. Wegwu[1] · Ebenezer O. Farombi[2]

Abstract

This study investigated the effects of ethanol (EtOH) on manganese (Mn)-induced striatal toxicity in rat by evaluating the neurobehavioral changes, biochemical and molecular events in rats exposed to Mn alone at 30 mg/kg, or their combination with EtOH at 1.25- and 5-g/kg body weight for 35 consecutive days. Locomotive and exploratory profiles were assessed using a video tracking software (ANY-Maze software) during a 5-min trial in a novel environment. Subsequently, acetylcholinesterase (AChE) activity, oxidative stress markers, histological morphology, and expression of apoptotic proteins (p53 and Bax and caspase-3) and anti-apoptotic protein (Bcl-2) were assessed in the striatum. Results showed that Mn, EtOH, and their combination induced locomotor and motor deficits. Track plot analysis indicated that EtOH exacerbated the Mn-induced reduction in exploratory profiles of exposed rats. Similarly, exposure of rats to Mn, EtOH, or combination of Mn and EtOH resulted in decreased activities of anti-oxidant enzymes, diminished level of reduced glutathione, downregulated Bcl-2 expression, increased AChE activity, enhanced hydrogen peroxide and lipid peroxidation levels, and upregulated expressions of p53, Bax, and caspase-3. Moreover, potentiation of Mn-induced striatal toxicity by EtOH co-exposure was dose dependent. Taken together, it seems that EtOH exacerbates Mn-induced neurobehavioral deficits, oxidative stress, and apoptosis induction via the regulation of p53, caspase-3, and Bax/Bcl-2 ratio-dependent pathway in rat striatum.

Keywords Manganese · Ethanol · Neurobehavioral deficits · Oxidative stress · Apoptosis · Striatum

Introduction

Manganese (Mn) is essential for many biological functions, albeit high level of Mn may accumulate in the basal ganglia structure and cause Manganism, a Parkinson-like syndrome characterized by bradykinesia, dystonia, rigidity, cognitive deficits, nervousness, and motor dysfunctions [1–6]. Occupational exposure to Mn include welding, mining, use of organochemical fungicide, and production of dry battery [7]. The molecular mechanism of Mn neurotoxicity has been studied in animal models to mimic the various forms of Mn exposure such as occupational, environmental, and parenteral nutrition. Also, Mn has been reported to induce dopaminergic neurodegeneration and microglial activation in substantia nigra of rat [8]. Available reports have established that Mn, through oxidative stress, may lead to activation of mitogen-activated protein kinase (MAPKs) both in vitro an in vivo [9–11].

Epidemiological data indicated that the time frame for symptoms appearance in humans overexposed to Mn is between 2 and 34 years (average 16.3 years). The symptoms include memory loss, headache and insomnia, exaggerated tendon reflexes, emotional instability, speech disturbances, hyper-myotonia, hand tremor, and festinating gait [12]. In severe cases, physical signs of Mn neurotoxicity include dystonic movement of the extremities with tremor and a particularly characteristic gait called "cockwalk" in which patients walk on their toes, leaning forward [12]. A Korean study that

✉ Kpobari W. Nkpaa
nkwilly@gmail.com

✉ Matthew O. Wegwu
matthew.wegwu@uniport.edu.ng

[1] Environmental Toxicology Unit, Department of Biochemistry, Faculty of Science, University of Port Harcourt, P.M.B 5323, Choba, Rivers State, Nigeria

[2] Drug Metabolism and Toxicology Research Laboratories, Department of Biochemistry, College of Medicine, University of Ibadan, Ibadan, Nigeria

followed 104,544 male workers exposed to Mn reported manifestation of extrapyramidal and movement disorders, the hallmark features of manganism after ≥ 10 years of chronic Mn exposure [13]. In early stages of manganism, upon cessation of Mn exposure, the symptoms might be reversed, while in patients with motor disturbances, manganism is irreversible [14]. However, influence of alcohol on Mn-associated toxicity on the basal ganglia and striatum is yet to be investigated, even in human.

According to the World Health Organization, alcohol is estimated as the fourth leading risk factor for global disability and death, a rank that is almost close to the mortality rate from tobacco [15]. Acute alcohol intoxication has been reported throughout history and remains one of the world's most widespread recreational drugs [16]. Adedara et al. [17] reported that African countries are ranked among the highest consumers of alcohol per capita. It has been shown that alcohol consumers in Africa tend to consume alcohol in high amount and more often [16]. This is particularly true when consumption of traditional and local alcoholic beverages is added to the estimates. Remarkably, consumption of spirits in developing African nations has been an assertion of sophistication and higher economic status [17]. However, alcohol induces neurodegeneration via induction of apoptosis and necrosis through activation of caspases [18] and inhibition of the electron transport chain. [19]. Simultaneous exposure to chemical mixtures via occupational, environmental, nutritional, and social settings continues to pose serious health challenges to humans. While people from southern Nigeria are known to consume high amount of alcohol on a regular basis, fishermen, farmers, and sand diggers from this geographical area are reported to be exposed to Mn in drinking water and food [16–22]. Hence, there is need to investigate the possible neurotoxicological effects (synergistic or antagonistic) of co-exposure to Mn and EtOH.

The striatum is one of the nuclei in the subcortical basal ganglia of the forebrain. It receives dopaminergic and glutamatergic inputs and serves as the primary input to the rest of the basal ganglion nuclei. It also coordinates multiple aspects of cognition, motor/locomotive function, action planning, motivation, decision-making, reinforcement, executive functions (e.g., inhibitory control), stimulus response, learning, and reward perception [23–26]. Alteration in striatal functions has been implicated in Parkinson's disease, Huntington's disease, choreas, choreoathetosis, dyskinesias, addiction, bipolar disorder, autism spectrum disorder, and dysfunction (depression and obsessive-compulsive disorder) [27–31]. Although the neurotoxicity of Mn on the basal ganglion nuclei and their connecting pathways has been extensively reported, the influence of EtOH on Mn-induced toxicity in the striatum is not yet understood. Therefore, the present study was designed to investigate the influence of EtOH on Mn-induced neurotoxicity by evaluating the neurobehavioral characteristics, biochemical profile, and molecular changes in striatum of rats.

Materials and Methods

Chemicals

Manganese chloride (as $MnCl_2.4H_2O$, $\geq 99.9\%$), acetylthiocholine iodide, 1-chloro-2,4-dinitrobenzene (CDNB), 5′,5′-dithio-bis-2-nitrobenzoic acid (DNTB; Elman's reagent), thiobarbituric acid (TBA), trichloroacetic acid (TCA), epinephrine, glutathione, and hydrogen peroxide were purchased from Sigma Chemical Co. (St. Louis, MO, USA). Rabbit polyclonal primary anti-p53, anti-Bax, anti-Bcl-2, anti-caspase-3, and anti-rabbit secondary antibody were obtained from Elabscience (China) and Abcam (UK). All other reagents were of highest analytical grade and were purchased from the British Drug Houses (Poole, Dorset, UK).

Animal Model

Fifty-five male Wistar rats (8 weeks; weighing 140–160 g) were obtained from the Central Animal House, College of Medicine, University of Ibadan, Ibadan, Oyo State. Animals were housed in standard polypropylene cages under room temperature 25 ± 2 °C with a 12-h light/dark cycles throughout the duration of the experiment and were fed on rat pellets obtained from Ladokun Feeds, Ibadan, with unlimited access to water. Prior to the commencement of the study, the animals were acclimatized for 2 weeks. The ethical approval was obtained from the University of Ibadan institutional Animal Care and Use Research Ethics Committee (ACUREC), and the experiment was conducted in accordance with the "Guide for the Care of Laboratory Animals" approved by the National Academy of Science (NAS).

Experimental Design

The rats were randomly divided to five groups of 11 rats each and were treated for 35 consecutive days as follows:

Group I (control): Rats received normal drinking water alone.

Group II (EtOH alone): Rats were orally treated with ethanol alone at 5-g/kg body weight.

Group III (Mn alone): Rats were orally treated with manganese alone at a dose of 30-mg/kg body weight.

Group IV (Mn + EtOH 1): Rats were orally co-treated with manganese at 30-mg/kg body weight and ethanol at 1.25-g/kg body weight.

Group V (Mn + EtOH 2): Rats were orally co-treated with manganese at 30-mg/kg body weight and ethanol at 5-g/kg body weight.

The doses of Mn (30 mg/kg) and EtOH (1.25 and 5 g/kg—40% *v/v*) used in this study were chosen based

on the results from pilot study in our laboratory and previously published data [21].

Behavioral Testing

Open-Field Test

The open-field test in a novel environment was conducted 24 h after the last administration of Mn and/or EtOH to investigate the neurobehavioral pattern of experimental rats according to standard procedure [32] with slight modification. The apparatus consisted of a square arena (56 cm in width × 56 cm in length × 20 cm in height) made of white wood with its floor subdivided into 16 squares that allow a perfect peripheral and central parts. The experimental rats (8 in each group) were randomly selected and subsequently placed in the center of the apparatus and allowed to explore the arena freely without distraction and the experimenter not allowed within visible range of the animals. The neurobehavioral profiles (behavioral end points), namely, maximum speed, total distanced traveled, total distance immobile, number of line crossing, grooming, rotation, and absolute turn angle, were recorded during a 5-min trial period using a webcam (a DNE webcam, Porto Alegre, Brazil) carefully positioned above the apparatus and attached to a laptop using Free2X webcam software. The experimental protocol was closely followed and conducted between the time period of 10.00 am and 4.00 pm in order to maintain the same experimental settings and conditions (similar manipulation, illumination, and time period). Necessary cares and cautions were taken when transferring the animal from their various group cages to the novel environment of the open-field apparatus to avoid stress-related handling. At the end of the experiment, the neurobehavioral parameters were computed automatically at a rate of 30 frames/s using a video-tracking software (ANY-maze, Stoelting, CO, USA).

Evaluation of Neurobehavioral Parameters

Exploratory and locomotor activities were analyzed in this study to demonstrate habituation to novelty stress. Exploratory activity in the novel environment was presented as habituation base using track plots. The habituation base during the trial sessions was defined as the space in the open box apparatus where the experimental animal has high occupancy preference from the start to end points of exploratory tours [33].

Forelimb Grip Test

The rats were suspended on a horizontal 4-mm-diameter metal rope with their forepaws. The metal rope was about 40 cm above a foam pad. The time taken for the animals to fall off the rope was video captured and recorded.

Negative Geotaxis

The experimental animals were placed head down on a 45° inclined board. The hind limbs of the animals were placed in the middle of the board. The time taken to turn around and climb up the board with their forelimbs reaching the upper rim was video captured and recorded.

Tissue Sampling

After the neurobehavioral trials, the experimental rats were weighed and sacrificed. The cranium was opened and the striatum was carefully dissected out. The brains of rats, three from each group, were fixed in 4% paraformaldehyde solution for histology and immunohistochemistry analyses. The remaining striatal tissues were homogenized in eight volumes of 50 mM Tris-HCl buffer (pH 7.4) containing 1.15% potassium chloride, and the resulting homogenate was centrifuged at $12,000 \times g$ for 15 min at 4 °C to obtain the post-mitochondrial fraction. The supernatant was subsequently used for biochemical determinations. Protein concentration was determined at 595 nm according to the method of Bradford [34].

Biochemical Assay

Measurement of Acetylcholinesterase Activity

Acetylcholinesterase (AChE) activity in the striatal tissue was assayed according to the method of Ellman et al. [35]. The assay mixture consisted of 110 μL of distilled water, 20 μL of 100 mM potassium phosphate buffer (pH 7.4), 20 μL of 10 mM DTNB, 30 μL of diluted sample, and 20 μL of 8 mM acetylthiocholine as a substrate. The degradation of acetylthiocholine iodide was analyzed at 412 nm spectrophotometrically for 5 min at 30-s intervals, and the results were expressed as μmol/min/mg protein.

Measurement of Superoxide Dismutase Activity

Superoxide dismutase (SOD) activity was assayed by measuring the inhibition of auto-oxidation of epinephrine at pH 10.2 (30 °C) according to the method of Misra and Fridovich [36]. In brief, 50 μL of the sample was added to 2.4 mL of 0.05 M carbonate buffer (pH 10.2) and the reaction was initiated by the addition of 60 μL of 0.3 M of freshly prepared epinephrine. The increase in absorbance at 480 nm was monitored for 150 s at 30-s intervals with the aid of UV-visible spectrophotometer. Reaction mixture without the enzyme was used as the blank. SOD values were expressed as nanomoles epinephrine oxidized/min/mg protein.

Measurement of Catalase Activity

Catalase (CAT) activity was assayed using hydrogen peroxide as substrate according to the method of Clairborne [37]. In brief, the assay medium, containing 1.8 mL of 50 mM phosphate buffer at pH 7.0, 180 μL of 19 mM of H_2O_2, and 20 μL sample, was allowed to run for 3 min at 30-s intervals with absorbance measured at 570 nm with a UV-visible spectrophotometer. CAT value was expressed as micromole H_2O_2 consumed/min/mg protein.

Measurement of Glutathione–S-Transferase Activity

Glutathione–S-transferase (GST) activity was assayed using CDNB as substrate according to the method of Habig et al. [38]. In brief, the reaction medium consisted of 300 μL of 0.1 M phosphate buffer (pH 6.5), 20 μL of 0.1 M reduced glutathione, and 40 μL of 20 mM of CDNB. This reaction mixture was later incubated for 5 min at 37 °C. The reaction was initiated by the addition of 40 μL of sample, and the absorbance was monitored for 5 min (30-s interval) at 340 nm. Reaction mixture without the enzyme was used as blank. GST enzyme activity was expressed as micromole of GSH-CDNB conjugate formed/min/mg protein.

Measurement of Glutathione Peroxidase Activity

Glutathione peroxidase (GPx) activity was assayed according to the method of Rotruck et al. [39]. In brief, the reaction mixture consisted 100 μL of 10 mM sodium azide, 200 μL of 4.0 mM GSH, 500 μL potassium phosphate buffer, 100 μL of 2.5 mM H_2O_2, and 50 μL of striatum sample. The total volume was made up to 2.0 mL with distilled water. The reaction mixture was incubated for 3 min at 37 °C. Subsequently, the reaction was terminated by adding 500 μL of 10% TCA. The residual glutathione level was determined by centrifuging the reaction mixture. The supernatant was thereafter removed, and to this, 2.0 mL of 0.3 M dipotassium hydrogen orthophosphate solution and 500 μL of DTNB reagent were added. The formed color was read at 412 nm. GPx activity was expressed as unit/mg protein.

Analysis of Reduced Glutathione Level

Reduced glutathione (GSH) level was determined by measuring the chromophoric complex formed between DTNB and endogenous glutathione at 412 nm according to the method of Beutler et al. [40]. In brief, 120 μL of sample was deproteinized by the addition of 120 μL of sulfosalicyclic acid (precipitating solution at 4%) and resulting solution was vortexed and centrifuged at 5000 rpm for 5 min. Thereafter, 150 μL of the supernatant was added to 450 μL of Elman's reagent. The quantity of GSH was proportional to the absorbance at 412 nm. Reaction mixture without the supernatant was used as blank. GSH level was expressed as micromole/mg protein.

Analysis of Hydrogen Peroxide Level

Hydrogen peroxide (H_2O_2) generation was determined according to the method of Wolff [41]. In brief, the ferrous oxidation with xylenol orange (FOX-1) reagent was prepared using 100 μmol/L xylenol orange, 100 μL sorbitol, 250 μmol/L ammonium ferrous sulfate, and 25 mmol/L of H_2SO_4. The assay mixture consisting 20 μL of the sample and 180 μL of FOX-1 reagent was vortexed and thereafter incubated at room temperature for 30 min. The absorbance was read at 560 nm. H_2O_2 concentration was obtained from a linear standard curve within a concentration range of 0–5 μmol/L. The level of H_2O_2 was expressed as micromole of H_2O_2/mg protein.

Measurement of Lipid Peroxidation Level

Lipid peroxidation (LPO) was determined by measuring the level of malondialdehyde (MDA), an end product of lipid peroxidation, according to the method described by Farombi et al. [42] with slight modification. In brief, the reaction mixture consisted of 150 μL of 0.1 M phosphate buffer, 50 μL of sample, 100 μL of 10% TCA, and 100 μL of 0.75% 2-thiobarbituric acid (TBA) in 0.1 mol/L HCl. The reaction mixture was heated at 90–95 °C for 30 min. After cooling at room temperature, they were centrifuged at 8000×g for 10 min and the absorbance of the supernatant was read against distilled water at 532 nm. The level of MDA was calculated using the extinction coefficient of 1.56×10^5 L/mol/cm and was expressed as the micromole MDA formed/mg protein.

Immunohistochemistry Analysis

Following sacrifice, the brain of each rat was immediately fixed overnight in 4% phosphate-buffered saline buffered formalin solution for 48 h and cryo-protected in 30% sucrose solution at 4 °C overnight before the striatum was dissected, embedded in paraffin block, and sectioned to a thickness of 5 μm using a RM2035 microtome (Reichert, Leica). The sectioned tissues were placed on a poly-L-lysine charged slides, cleared in xylene, dehydrated in graded series of alcohol rinses (100–50%), and then placed in PBS (pH 7.6). Antigen retrieval was performed by boiling for 20 min in a citrate buffer (0.1 M). Sections were then treated with 3% hydrogen peroxide for 15 min to quench endogenous peroxidase activity. All slides were subsequently incubated overnight at 4 °C with rabbit anti-p53, anti-Bax, anti-Bcl-2, and anti-caspase-3 polyclonal primary antibodies. All antibodies were added at 1:200 dilutions. After washing, the slides were overlaid with biotin-labeled secondary antibody and incubated at 23 °C in a moist

chamber for 1 h. Detection of the antibody was performed using a streptavidin-horseradish peroxidase detection system. Immune complexes were visualized using 3,3′-diaminobenzidine (DAB) as the chromogen. Thereafter, the specific staining on the striatal tissues were observed with the aid of a light microscopy (SP-98-FL, Inverted Fluorescent Microscope, Brunel Microscope Limited) that is coupled with a high-resolution camera (Canon EOS 1100D, Japan). The generated images were analyzed and processed with an open-source Fiji-ImageJ Software (v1.51a NIH). Six micrographs from each of the representative groups were analyzed with ImageJ. These images were deconvolved to filter microscope-associated noise while the color threshold was adjusted to a positive DAB stain region. The resultant images generated were further evaluated to obtain the mean intensity of immunoreactivity after removing the background intensity representing the total intensity of the image. The data were expressed as percentage (%) of high positive DAB intensity.

Histological Examination

Buffered formalin fixed brain samples processed for histological examination according to established procedure by Bancroft and Gamble [43]. In brief, the fixed striatum was dehydrated in increasing concentrations of alcohol, cleared by xylene, and embedded in paraffin wax. Thereafter, the tissues were cut with a microtone at 5-μm sections, fixed on slides, and stained with hematoxylin and eosin. All slides were coded before viewing with light microscope (SP-98-FL, Inverted Fluorescent Microscope, Brunel Microscope Limited) that is coupled with a high-resolution camera (Canon EOS 1100D, Japan) by a neuroanatomist.

Statistical Analysis

Statistical analyses were carried out using two-way analysis of variance (ANOVA) for multiple comparison to compare the experimental groups followed by Bonferroni's post hoc test using GraphPad Prism 6 software (version 5; GraphPad Software, La Jolla, CA, USA). Values of $p < 0.05$ were considered statistically significant.

Results

Effect of EtOH and Mn Co-Exposure on the General Health Status, Locomotor, and Motor Activities

Rats exposed to EtOH and Mn combinations showed physical changes such as hair loss, weight loss, tremors, changes in respiratory rate, and discharges from the eyes and nose within and beginning from day 31 (data not shown). The results of motor and locomotor performance during a 5-min trial in a novel environment are presented in Figs. 1 and 2. Rats administered Mn alone, EtOH alone, and their combination showed significant ($p < 0.05$) decrease in maximal speed, total
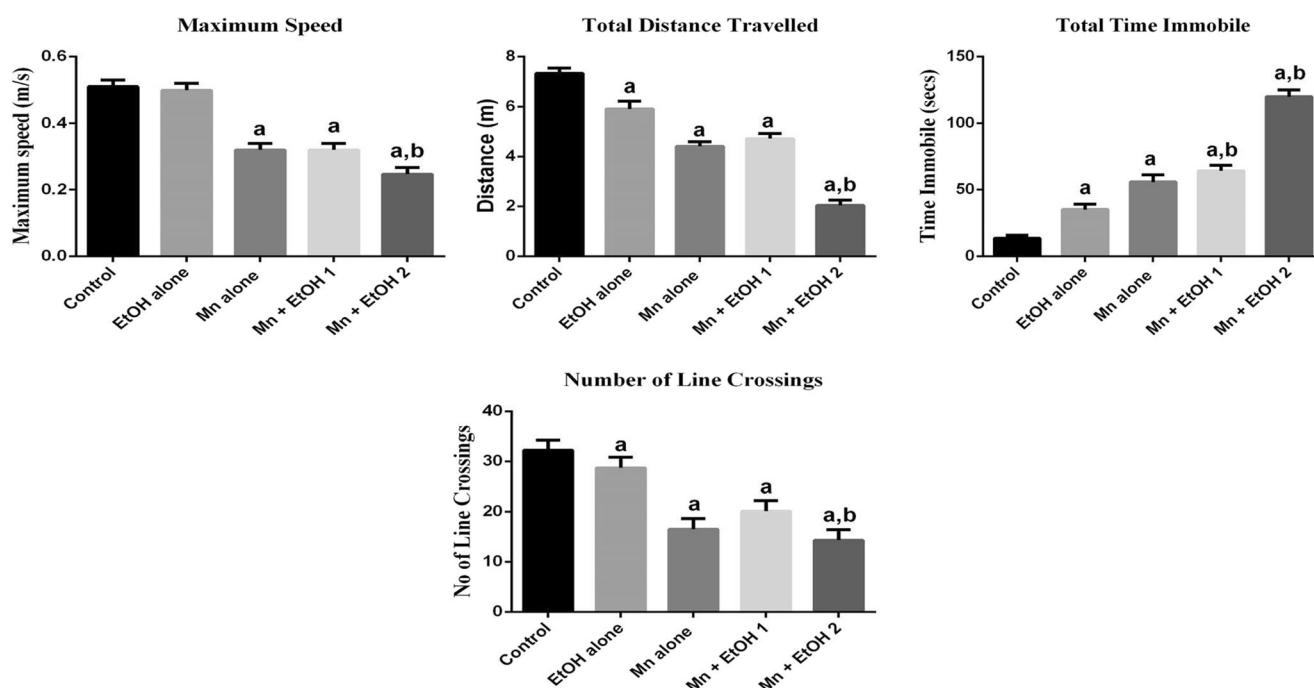

Fig. 1 The effect of co-exposure of manganese and ethanol on locomotion activities of rats. Manganese, Mn; ethanol, EtOH; Mn (30 mg/kg body weight); EtOH 1 (1.25 g/kg body weight); EtOH 2 (5 g/kg body weight). The figure depicts the influence of Mn an EtOH exposure on maximum speed, total distance traveled, total time immobile, and number of line crossings during a 5-min trial. The data are expressed as mean ± S.D. for 12 rats per group. **a** Values differ significantly from control ($p \leq 0.05$). **b** Values differ significantly from Mn alone at $p \leq 0.05$
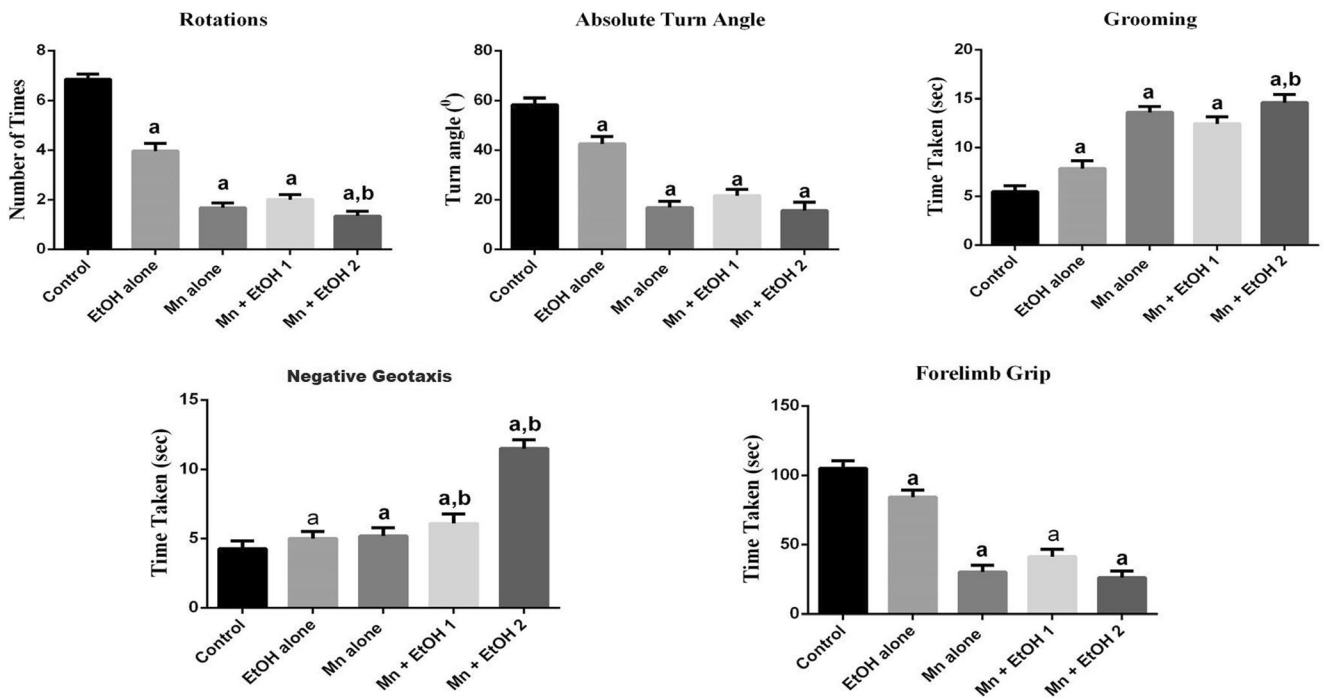
Fig. 2 The effect of co-exposure of manganese and ethanol on locomotion and motor activities of rats. Manganese, Mn; ethanol, EtOH; Mn (30 mg/kg body weight); EtOH 1 (1.25 g/kg body weight); EtOH 2 (5 g/kg body weight). The figure depicts the influence of Mn an EtOH exposure on body rotation, absolute turn angle, grooming, negative geotaxis, and forelimb grip during a 5-min trial. The data are expressed as mean ± S.D. for 12 rats per group. **a** Values differ significantly from control ($p \leq 0.05$). **b** Values differ significantly from Mn alone at $p \leq 0.05$

distance traveled, number of line crossing, body rotation, and absolute turn angle when compared to the control, whereas

grooming and total time immobile significantly ($p < 0.05$) increased when compared with the control. Moreover, co-
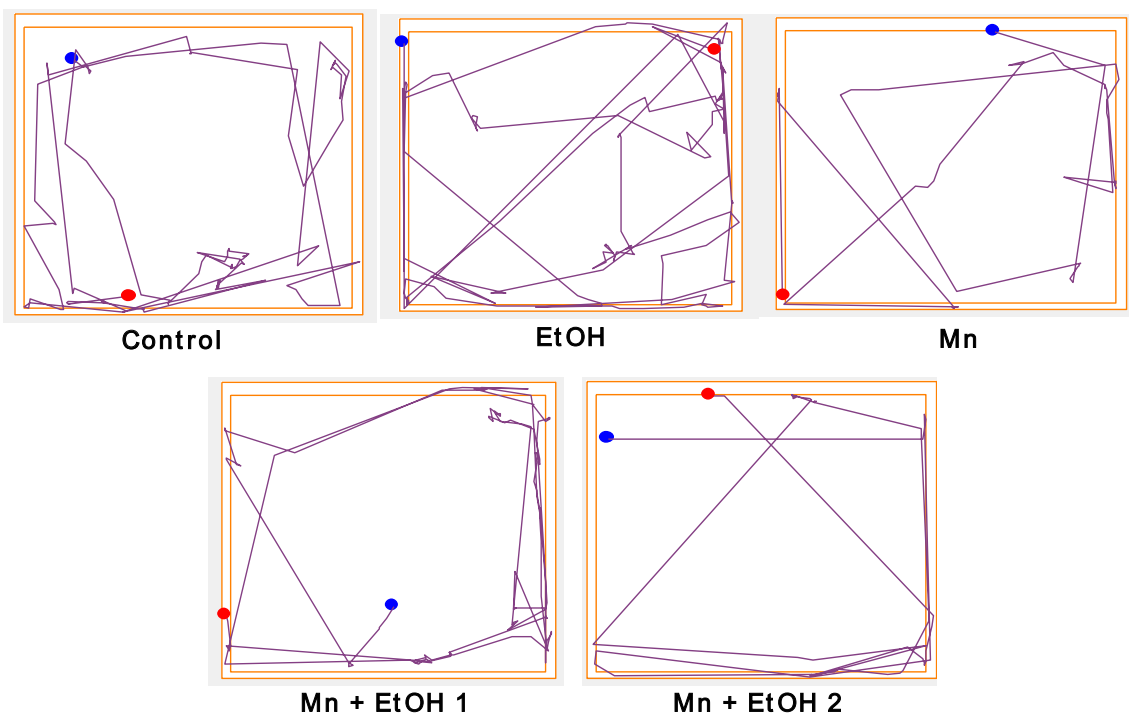

Fig. 3 Effect of co-exposure of manganese and ethanol on exploratory profiles represented by track plots during a 5-min trial. Mn = manganese, EtOH = ethanol. Mn (30 mg/kg body weight), EtOH 1 (1.25 g/kg body weight), EtOH 2 (5 g/kg body weight). The track plots represent the path traveled by rats in the novel apparatus. The video recorded were analyzed using video-tracking software (ANY-maze, Stoelting, CO, USA)
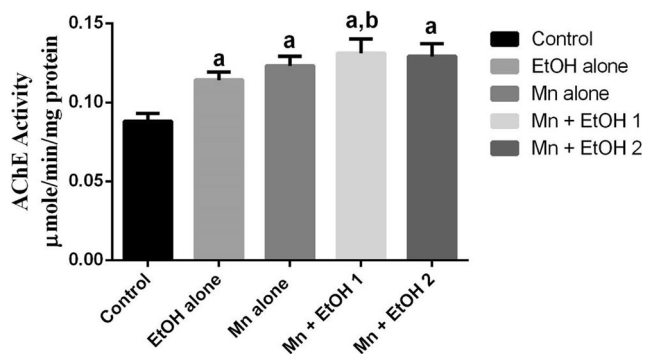
Fig. 4 The effect of co-exposure of manganese and ethanol on AChE activity in the striatum of rats. Manganese, Mn; ethanol, EtOH; Mn (30 mg/kg body weight); EtOH 1 (1.25 g/kg body weight); EtOH 2 (5 g/kg body weight). The data are expressed as mean ± S.D. for 8 rats per group. **a** Values differ significantly from control ($p \leq 0.05$). **b** Values differ significantly from Mn alone at $p \leq 0.05$

exposure of Mn and EtOH (i.e., Mn + EtOH 1 and Mn + EtOH 2) further exacerbated the decrease in maximal speed, total distance traveled, number of line crossing, body rotation, and absolute turn angle by 52%, 72%, 56%, 80%, and 73%, respectively, whereas Mn + EtOH 2 exacerbated the increase in grooming and total time immobile by 167% and 789%, respectively.

The influence of Mn alone, EtOH alone, and their combination on the negative geotaxis, forelimb grip, and time of grooming is presented in Fig. 2. Rats exposed to Mn alone, EtOH alone, and their combination exhibited a significant increase in the time taken to turn around and climb up an

inclined board (negative geotaxis) with their forelimbs reaching the upper rim than the control; ethanol aggravated the time taken to re-orient in dose-dependent manner. Furthermore, rats treated with Mn alone, EtOH alone, and their combination hung on the metal rope for shorter duration when compared with the control rats.

Effect of EtOH on Mn-Induced Exploratory Profile Alteration in Rats

The exploratory profile was monitored using video-tracking software (ANY-Maze, 6.0) during a 5-min trial in a novel environment. Figure 3 shows the representative track plots of the exploratory pattern of control rats and those treated with Mn alone, EtOH alone, and their combination within the open-box apparatus (novel environment). The control rats presented a usual behavioral profile pattern by walking around the apparatus, whereas the pattern of the track plots of rats exposed to Mn alone, EtOH alone, and their combination seemed to be significantly lower. Furthermore, EtOH exposure (Mn + EtOH) further exacerbated Mn-induced reduction in the density of the of track plots significantly when compared with the control. Interestingly, ethanol-treated animals seemed to exhibit enhanced impairment in judgment and risky behavior as they crossed over the middle of the apparatus more than the co-exposed rats. This may indicate that co-exposure to Mn and EtOH may affect EtOH-associated risky behavior possibly because of Mn + EtOH-induced hypokinesia as evident in Fig. 1.
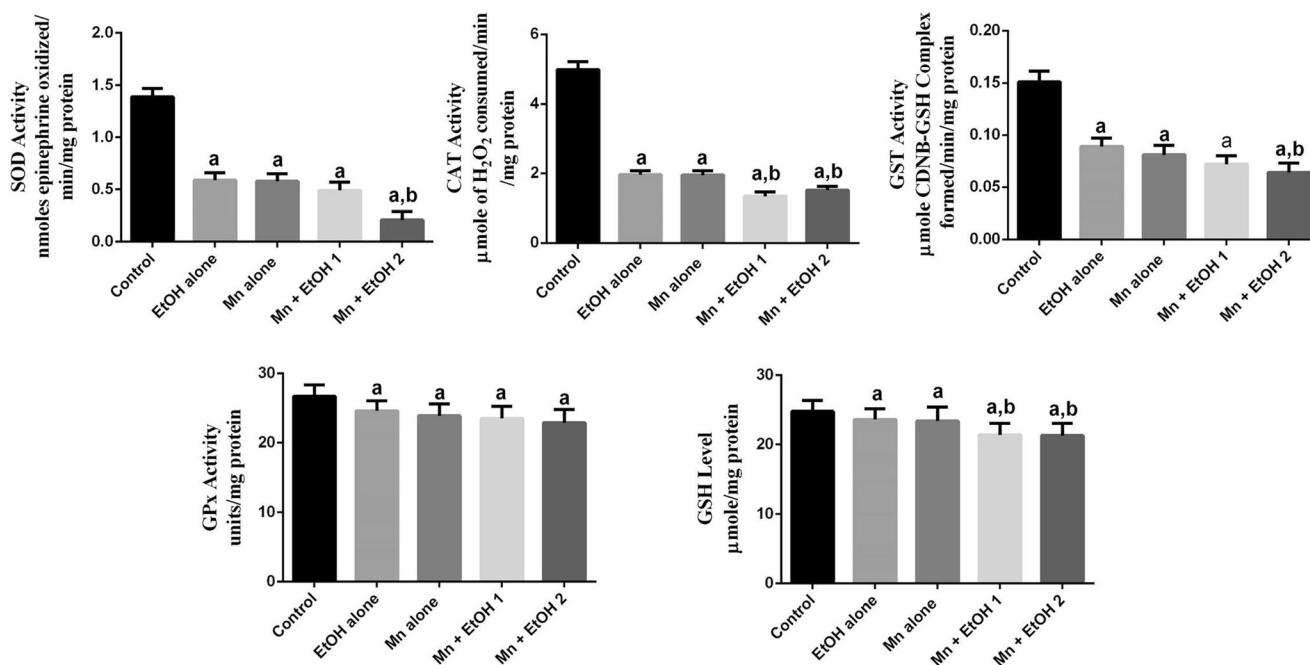

Fig. 5 The effect of co-exposure of manganese and ethanol on antioxidant enzyme activities (SOD, CAT, and GST and GPx) as well as the GSH level in the striatum of rats. Manganese, Mn; ethanol, EtOH; Mn (30 mg/kg body weight); EtOH 1 (1.25 g/kg body weight); EtOH 2 (5 g/kg body weight). The data are expressed as mean ± S.D. for 8 rats per group. **a** Values differ significantly from control ($p \leq 0.05$). **b** Values differ significantly from Mn alone at $p \leq 0.05$
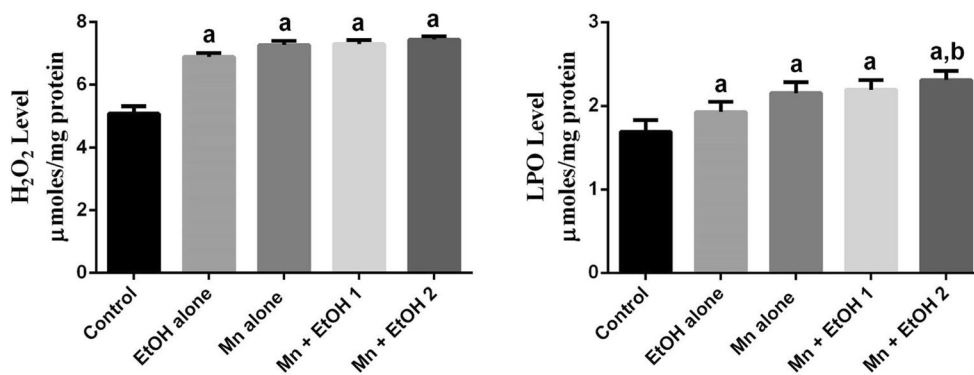
Fig. 6 The effect of co-exposure of manganese and ethanol on H_2O_2 and LPO levels in the cerebellar cortex of rats. Manganese, Mn; ethanol, EtOH; Mn (30 mg/kg body weight); EtOH 1 (1.25 g/kg body weight); EtOH 2 (5 g/kg body weight). The data are expressed as mean ± S.D. for 8 rats per group. **a** Values differ significantly from control ($p \leq 0.05$). **b** Values differ significantly from Mn alone at $p \leq 0.05$

Effect of EtOH on Mn-Induced Increases in Acetylcholinesterase Activity in the Striatum of Rats

The effect of Mn and EtOH exposure on AChE activity in the striatum of rats is presented in Fig. 4. Exposure to Mn alone, EtOH alone, and their combination resulted in a significant ($p < 0.05$) increase in AChE activity in the striatum of the treated rats. The percent increases in the AChE activity in the striatum were 30%, 40%, 49%, and 47% for EtOH alone, Mn alone, Mn + EtOH 1, and Mn + EtOH 2, respectively.

The Effect of EtOH on Mn-Induced Altered Antioxidant Status in the Striatum of Rats

Figure 5 depicts the effect of Mn alone, EtOH alone, and their combination on the antioxidant enzyme activities (SOD, CAT, GST, and GPx) as well as GSH level in the striatum of rats. Exposure to Mn alone, EtOH alone, and their combination caused a significant decrease in SOD and CAT activity in the striatum of the treated rats when compared to the control. Moreover, exposure of Mn alone, EtOH alone, and their combination significantly decreased the level of GSH and enzyme
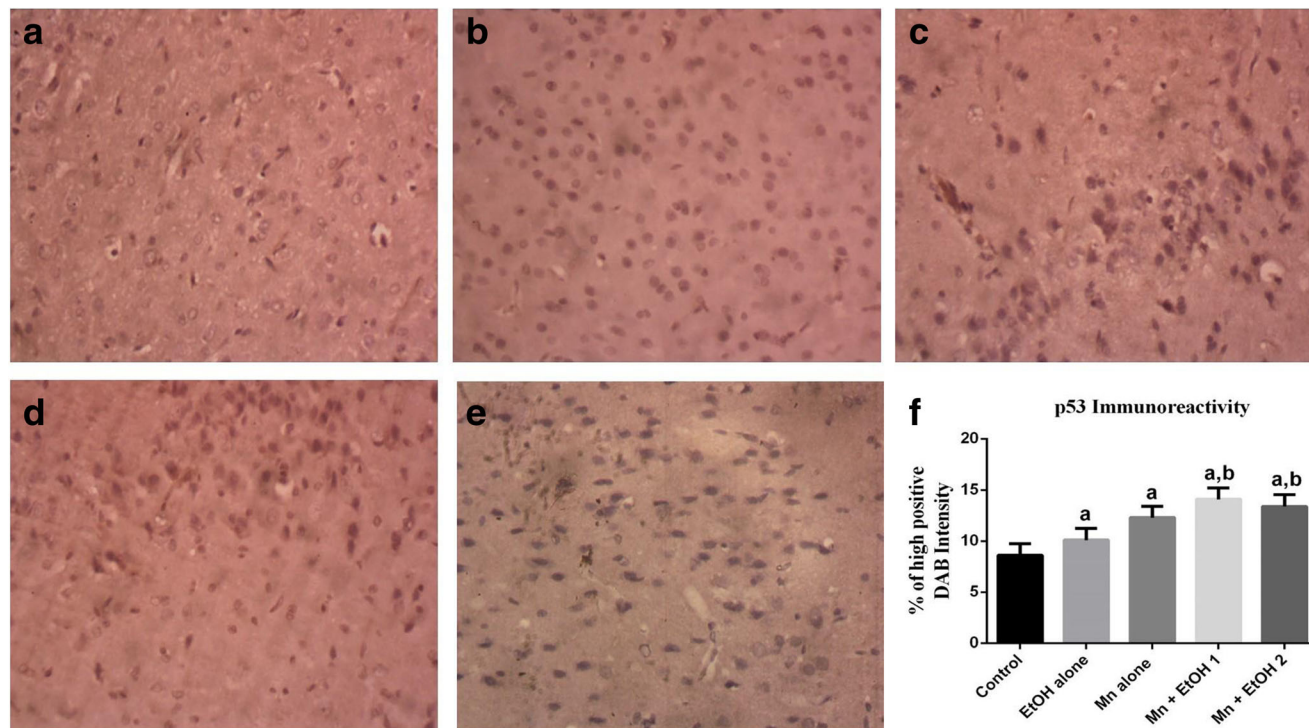

Fig. 7 Immunohistochemical staining showing the effect of Mn and EtOH on p53 protein expression in the striatum of rats' brain. A = control, B = EtOH, C = Mn, D = Mn + EtOH 1, E = Mn + EtOH 2. Manganese, Mn; ethanol, EtOH; Mn (30 mg/kg body weight); EtOH 1 (1.25 g/kg body weight); EtOH 2 (5 g/kg body weight). F = quantification of p53 protein expression in rat striatum. The data are expressed as mean ± S.D. for 3 rats per group. **a** Values differ significantly from control ($p \leq 0.05$). **b** Values differ significantly from Mn alone at $p \leq 0.05$
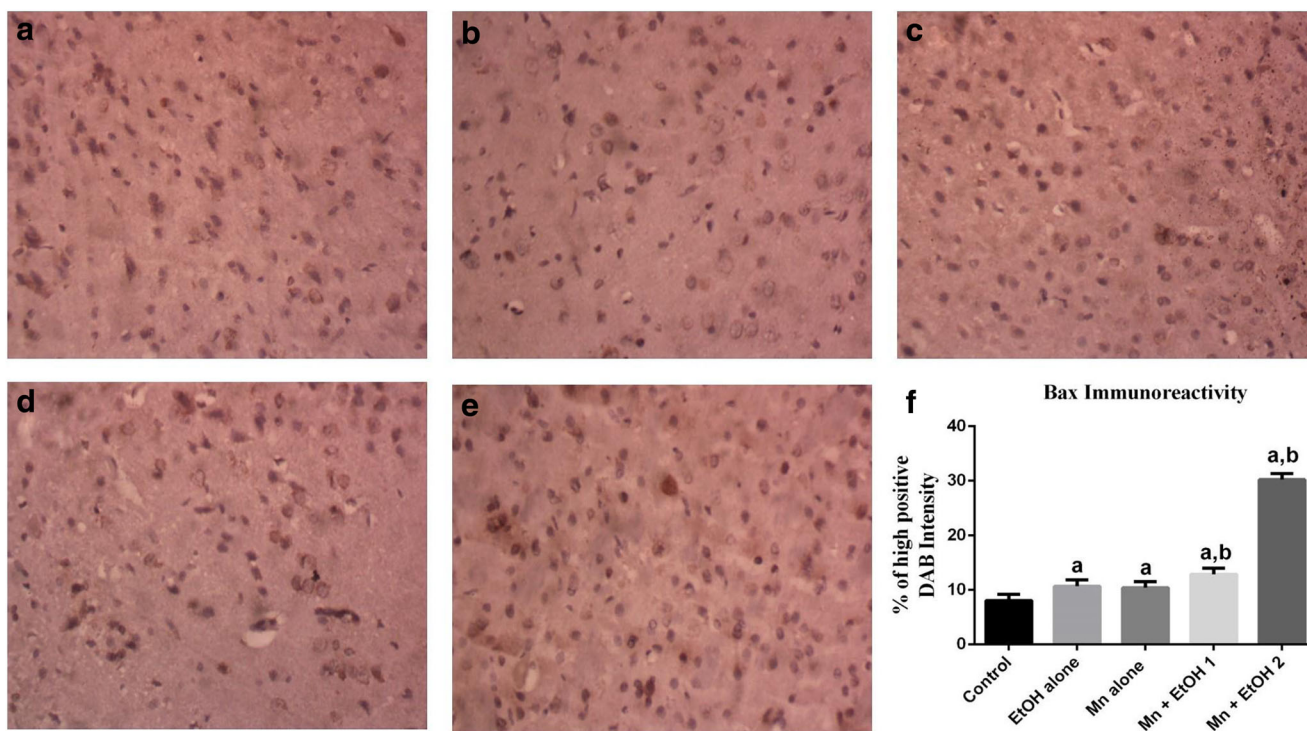
Fig. 8 Immunohistochemical staining showing the effect of Mn and EtOH on Bax protein expression in the striatum of rats' brain. A = control, B = EtOH, C = Mn, D = Mn + EtOH 1, E = Mn + EtOH 2. Manganese, Mn; ethanol, EtOH; Mn (30 mg/kg body weight); EtOH 1 (1.25 g/kg body weight); EtOH 2 (5 g/kg body weight). F = quantification of Bax protein expression in rat striatum. The data are expressed as mean ± S.D. for 3 rats per group. **a** Values differ significantly from control ($p \leq$ 0.05). **b** Values differ significantly from Mn alone at $p \leq 0.05$

Fig. 9 Immunohistochemical staining showing the effect of Mn and EtOH on Bcl-2 protein expression in the striatum of rats' brain. A = control, B = EtOH, C = Mn, D = Mn + EtOH 1, E = Mn + EtOH 2. Manganese, Mn; ethanol, EtOH; Mn (30 mg/kg body weight); EtOH 1 (1.25 g/kg body weight); EtOH 2 (5 g/kg body weight). F = quantification of Bcl-2 protein expression in rat striatum. The data are expressed as mean ± S.D. for 3 rats per group. **a** Values differ significantly from control ($p \leq 0.05$). **b** Values differ significantly from Mn alone at $p \leq 0.05$
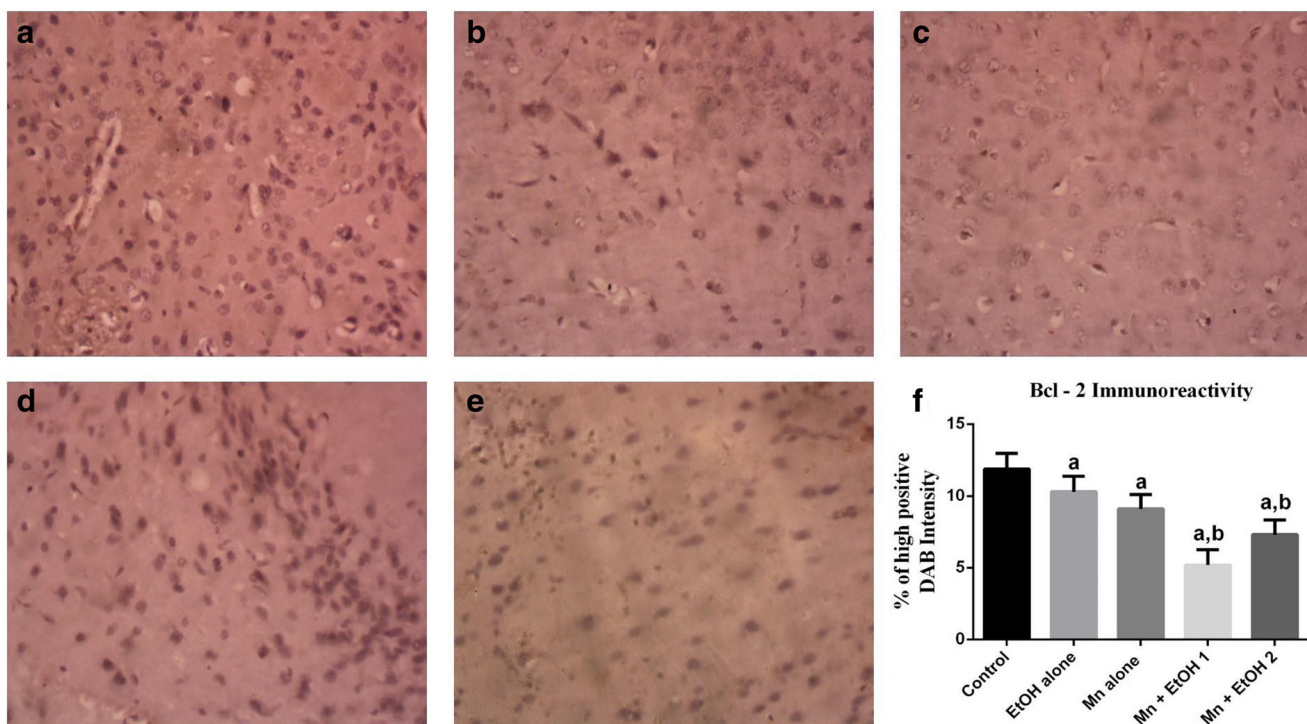
activities of GST and GPx when compared to the control. The effect of ethanol on Mn-induced changes in the aforementioned indices of antioxidant status was dose dependent.

Figure 6 depicts the effect of Mn alone, EtOH alone, and their combination on oxidative stress biomarkers (H_2O_2 and LPO) in striatum of rats. Exposure of rats to EtOH alone, Mn alone, Mn + EtOH 1, and Mn + EtOH 2 resulted in a significant increase in H_2O_2 generation and lipid peroxidation (LPO) in the striatum of rats when compared to the control group. The percent increases in H_2O_2 level were 35%, 43%, 43%, and 48% for EtOH alone, Mn alone, Mn + EtOH 1, and Mn + EtOH 2, respectively, whereas LPO level increased by 14%, 27%, 30%, and 37%, respectively.

The Effect of EtOH on Mn-Induced Apoptosis in Rat Striatum

Figures 7, 8, 9, and 10 depict the effect of Mn alone, EtOH alone, and their combination on pro-apoptotic and anti-apoptotic proteins (p53, Bax, Bcl-2, and caspase-3) in striatum of rats. Pro-apoptotic protein expressions (p53, Bax, and caspase-3) were upregulated in rat striatum exposed to Mn alone, EtOH alone, and their combination when compared to the control. p53, Bax, and caspase-3 protein expression in rat striatum exposed to Mn alone and EtOH alone exhibited weak immunoreactivity when compared to the co-exposed groups (i.e., Mn + EtOH 1 and Mn + EtOH 2), the later exhibited intense immunoreactivity. Moreover, Mn + EtOH 2 exacerbates the upregulation of protein expression of p53, Bax, and caspase-3 protein expressions in rat striatum compared to the Mn alone and EtOH alone. Furthermore, anti-apoptotic protein expression (Bcl-2) was downregulated in rats striatum exposed to Mn alone, EtOH alone, and their combination when compared with the control. Mn + EtOH 1 and Mn + EtOH 2 treatment exacerbated the downregulation of protein expression of Bcl-2 protein expression when compared with Mn alone and EtOH alone in rat striatum

Histopathological Changes in the Striatum of Rat Co-Exposed to Mn and EtOH

The histopathological alteration after co-exposure to Mn and EtOH is shown in Fig. 11. The striatum of the control rats appeared structurally and functionally normal with the neurons exhibiting open chromatin pattern. The experimental rats treated with Mn alone, EtOH alone, or their combination showed pathological features in the striatum. The histopathological sections showed marked neuronal degeneration as shown by the scattered dark and red neurons suggesting neuronal degeneration especially in the Mn + EtOH 1 and the Mn + EtOH 2 groups.
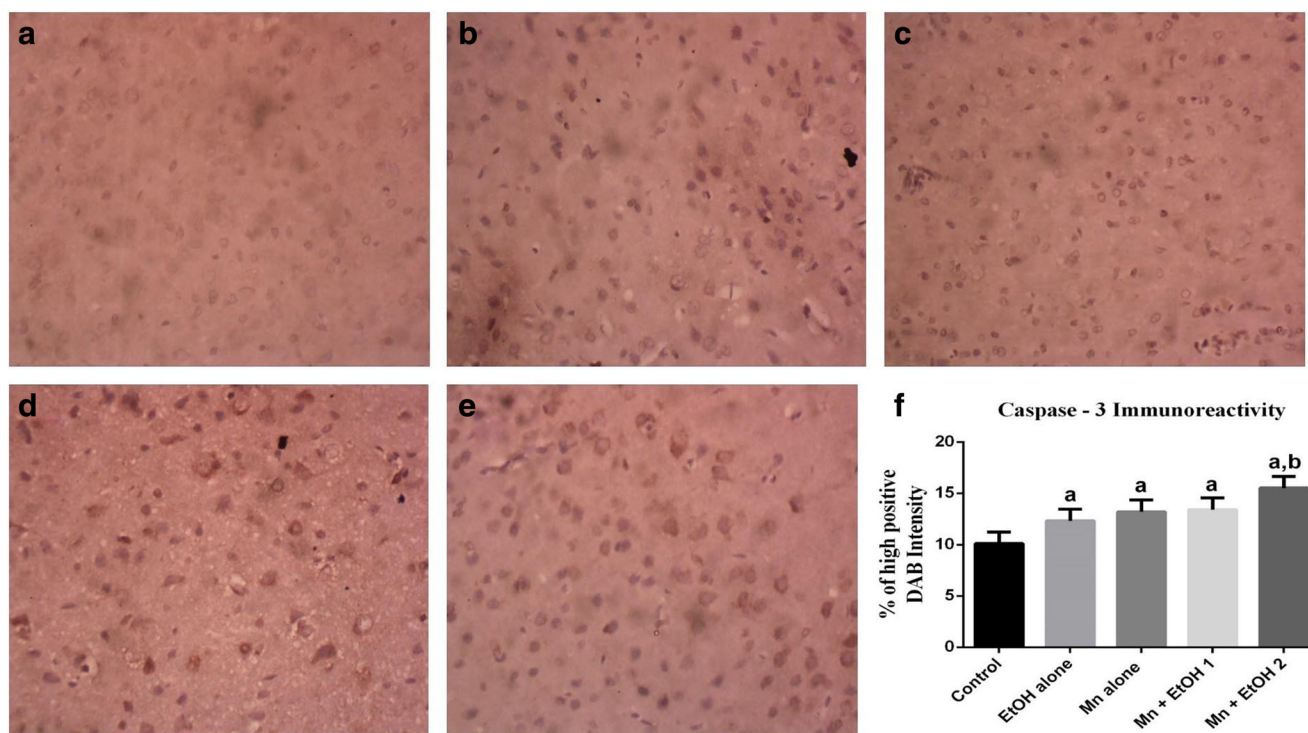

Fig. 10 Immunohistochemical staining showing the effect of Mn and EtOH on caspase-3 protein expression in the striatum of rats' brain. A = control, B = EtOH, C = Mn, D = Mn + EtOH 1, E = Mn + EtOH 2. Manganese, Mn; ethanol, EtOH; Mn (30 mg/kg body weight); EtOH 1 (1.25 g/kg body weight); EtOH 2 (5 g/kg body weight). F = quantification of caspase-3 protein expression in rat striatum. The data are expressed as mean ± S.D. for 3 rats per group. **a** Values differ significantly from control ($p \leq 0.05$). **b** Values differ significantly from Mn alone at $p \leq 0.05$
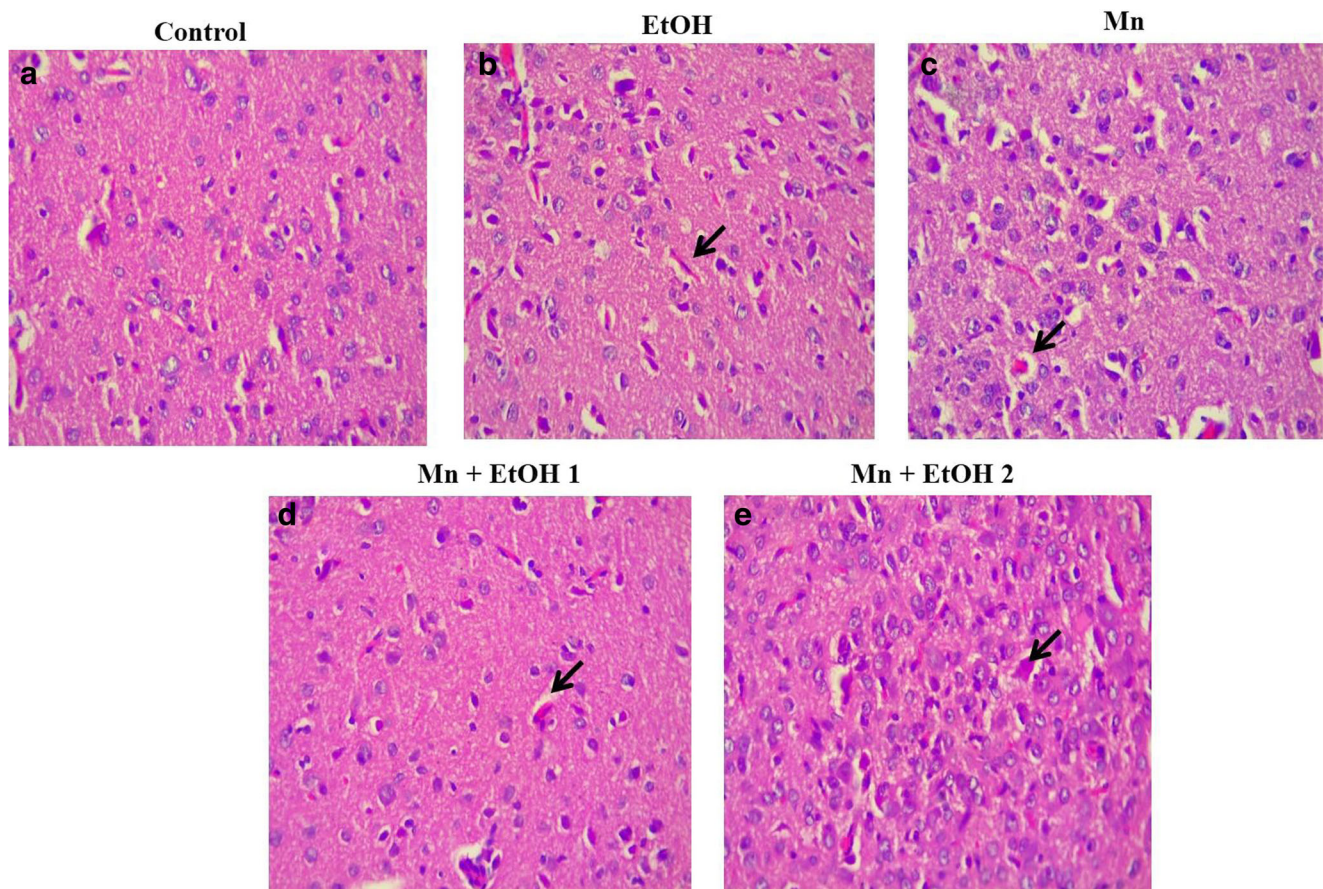
Fig. 11 Representative histopathological sections of striatum. The striatum of rats from the control showing normal morphology. The striatum of rats treated with Mn alone, EtOH alone, and in combination showing marked neuronal degeneration (black arrow). Manganese, Mn; ethanol, EtOH; Mn (30 mg/kg body weight); EtOH 1 (1.25 g/kg body weight); EtOH 2 (5 g/kg body weight). H&E stain. Magnification ×400

Discussion

Although Mn is an essential trace element, exposure to excessive of it can cause a variety of neurotoxic effects mediated by alterations in oxidative stress biomarkers, inflammation, and apoptosis induction, particularly in the striatum [44]. Deregulation of striatal functions has been implicated in a number of neurodegenerative diseases [27]. Given the penchant of workers in many parts of the world, most especially in developing nations, for consuming alcohol in large amount [15], and exposure of same individuals to Mn through occupation, environmental contamination, and drinking water [7], we evaluated the neurobehavioral changes and biochemical and molecular events in the striatum of rats exposed to Mn and co-exposed to low and high doses of ethanol. In our experiments, we showed that EtOH exacerbated Mn-induced neurobehavioral deficits, oxidative stress, and apoptosis induction.

Investigation of neurobehavioral profile has been an established protocol for the assessment or characterization of the effect of various toxic compounds on motor and locomotor activities in animal models [32]. Our findings indicate that

EtOH exacerbates Mn-induced disruption in coordination, decrease in exploratory profile, and marked reduction in the absolute turn angle and body rotation. The disorganization of behavioral pattern of the experimental rats may be due to alteration in the motor posture pattern, disruption between muscular junctions and nervous system, and the suppression of spontaneous motor activities in the exposed animals [45, 46]. Neurobehavioral functions and regulatory activity of AChE are well documented [47]. AchE is one of the two enzymes involved in cellular maintenance of acetylcholine (ACh), a neurotransmitter of the cholinergic system [48]. We observed that exposure to Mn alone and EtOH alone resulted in a significant increase in AChE activity in the striatum of rats, and this was exacerbated by Mn and EtOH co-exposure. Our result agrees with previous findings that demonstrated enhanced AChE activity upon Mn exposure [33, 49, 50]. Increase AChE activity may decrease acetylcholine levels in the synaptic cleft and impair motor, locomotor, and exploratory activities [48, 50]. This may be responsible for the behavioral deficits observed in the exposed rats in this study.

Several reports have established a direct connection between inflammation, oxidative stress, and neurotoxicity

[51–54]. In connection to this, striatum has been demonstrated to be more vulnerable to oxidative assault [55]. The reactive oxygen species (ROS)-scavenging enzymes—SOD, CAT, GST, and GPx—all play a major role in regulating the intracellular concentration of ROS. In the present study, there was a significant reduction in the activities of striatal antioxidant enzymes and level of GSH in Mn alone, EtOH alone, and their combination. This indicates a state of oxidative stress possibly due to inhibition of the radical detoxifying systems in the striatum of the exposed rats. Several studies have shown that significant increase in the formation of lipid peroxidation and H_2O_2 confirmed oxidative stress [33, 56]. EtOH may be enhancing free radical and peroxyl radical generation, which damages the lipid membranes, thereby leading to lipid peroxidation and subsequent neurodegeneration in the striatum.

The gene expression of Bax is regulated by p53 and has been shown to be implicated in p53-mediated apoptosis [57]. Translocation of p53 from the cytosol to the mitochondria disrupts Bcl-2/Bax ratio, which ultimately results in apoptosis induction mediated by the release of cytochrome C, activation of caspases, and other pro-apoptotic factors [58, 59]. On the other hand, Bcl-2, located on the outer mitochondrial membrane, promotes cellular survival, by inhibiting pro-apoptotic proteins, thereby suppressing induction apoptotic cascade [60]. Thus, the level of Bcl-2 versus Bax determines the resistance of cell to apoptosis [61]. In the present study, expressions of pro-apoptotic proteins (p53, Bax, and caspase-3) were upregulated while anti-apoptotic protein (Bcl-2) was downregulated in rat striatum exposed to Mn alone, EtOH alone, and their combination when compared to the control. It is pertinent to note that EtOH exacerbated Mn-induced upregulation of pro-apoptotic proteins and downregulation of anti-apoptotic protein when compared with Mn alone and EtOH alone. The upregulation of Bax and caspase-3 and downregulation of Bcl-2 expressions suggest the involvement of striatal apoptosis mediated by p53-related mechanism in the striatal neuronal degeneration of rats exposed to Mn and EtOH.

Conclusion

Taken together, reduced antioxidant enzymes activities and GSH level, enhanced lipid peroxidation, increased H_2O_2 production, changes in intracellular signaling of p53, activation of Bax and caspase-3, and downregulation of Bcl-2 may have contributed to the evident motor and locomotor impairment, oxidative stress, and striatal degeneration associated with the exacerbation of manganese-induced toxicity by ethanol. Therefore, Mn and EtOH co-exposure may result in neurodegeneration of the striatum, thereby leading to movement disorder-associated disease conditions.

References

1. Aschner M, Aschner JL (1991) Manganese neurotoxicity: cellular effects and blood–brain barrier transport. Neurosci Biobehav Rev 15:333–340

2. Erikson KM, Syversen T, Steinnes E, Aschner M (2004) Globus pallidus: a target brain region for divalent metal accumulation associated with dietary iron deficiency. J Nutr Biochem 15: 335–341

3. Cersosimo MG, Koller WC (2006) The diagnosis of manganese-induced parkinsonism. Neurotoxicology 27:340–346

4. Bouchard M, Mergler D, Baldwin M, Panisset M, Roels HA (2007) Neuropsychiatric symptoms and past manganese exposure in a ferro-alloy plant. Neurotoxicology 28:290–297

5. Guilarte TR, Burton NC, Verina T, Prabhu VV, Becker KG, Syversen T, Schneider JS (2008) Increased APLP1 expression and neurodegeneration in the frontal cortex of manganese-exposed non-human primates. J Neurochem 105: 1948–1959

6. Peres TV, Eyng H, Lopes SC, Colle D, Goncalves FM, Venske DKR, Lopes MW, Ben J, Bornhorst J, Schwerdtle T, Aschner M, Farina M, Prediger RD, Leal RB (2015) Developmental exposure to manganese induces lasting motor and cognitive impairment in rats. NeuroToxicology 50:28–37

7. Bowler RM, Gysens S, Diamond E, Nakagawa S, Drezgic M, Roels HA (2006) Manganese exposure: neuropsychological and neurological symptoms and effects in welders. Neurotoxicology 27:315–326

8. Zhao F, Cai T, Liu M, Zheng G, Luo W, Chen J (2009) Manganese induces dopaminergic neurodegeneration via microglial activation in a rat model of manganism. Toxicol Sci 107:156–164

9. Hirata Y, Furuta K, Miyazaki S, Suzuki M, Kiuchi K (2004) Anti-apoptotic and pro-apoptotic effect of NEPP11 on manganese-induced apoptosis and JNK pathway activation in PC12 cells. Brain Res 1021:241–247

10. Ito Y, Oh-hashi K, Kiuchi K, Hirata Y (2006) p44/42 MAP kinase and c-Jun Nterminal kinase contribute to the up-regulation of caspase-3 in manganese-induced apoptosis in PC12 cells. Brain Res 1099:1–7

11. Cordova F, Aguiar Jr, A, Peres T, Lopes M, Goncalves F, Pedro D, Lopes S, Pilati C, Prediger RS, Farina M, Erikson K, Aschner M, Leal R (2013) Manganese-exposed developing rats display motor deficits and striatal oxidative stress that are reversed by Trolox. Arch Toxicol 87:1231–1244

12. Benedetto A, Au C, Aschner M (2009) Manganese-induced dopaminergic neurodegeneration: insights into mechanisms and genetics shared with Parkinson's disease. Chem Rev 109(10):4862–4884

13. Yoon JH, Ahn YS (2015) A large, nationwide, longitudinal study of central nervous system diseases among Korean workers exposed to manganese. Parkinsonism Relat Disord 21(3):194–198

14. Crossgrove J, Zheng W (2004) Manganese toxicity upon overexposure. NMR Biomed 17:544–553

15. World Health Organization (2002) Reducing risks, Promoting Healthy Life 2002. The World Health Report, Geneva

16. World Health Organization (2004) Global status report on alcohol 2004. Geneva

17. Adedara IA, Owumi SE, Uwaifo AO, Farombi EO (2010) Aflatoxin B1 and ethanol co-exposure induces hepatic oxidative damage in mice. Toxicol Ind Health 26:717–724

18. Obernier JA, Bouldin TW, Crews FT (2002) Binge ethanol exposure in adult rats causes necrotic cell death. Alcohol Clin Exp Res 29:547–557

19. Hoek JB, Cahill A, Pastorino JG (2002) Alcohol and mitochondria: a dysfunctional relationship. Gastroenterology 122:2049–2063

20. Nkpaa KW, Patrick-Iwuanyanwu KC, Wegwu MO, Essien EB (2016) Health risk assessment of hazardous metals for population via consumption of seafood from Ogoniland, Rivers state, Nigeria; a case study of Kaa, B-dere, and Bodo City. Environ Monit Assess 188(1):9

21. Nkpaa KW, Amadi BA, Adedara IA, Wegwu MO, Farombi EO (2018) Ethanol exacerbates manganese – induced functional alterations along the hypothalamic-pituitary-gonadal axis of male rats. Neurosci Lett 684:47–54

22. Nkpaa KW, Amadi BA, Wegwu MO (2018a) Hazardous metals levels in groundwater from Gokana, Rivers state, Nigeria: non-cancer and cancer health risk assessment. Hum Ecol Risk Assess 24(1):214–224

23. Malenka RC, Nestler EJ, Hyman SE (2009) In: Sydor A, Brown RY (eds) Molecular neuropharmacology: A Foundation for clinical neuroscience, 2nd edn. McGraw-Hill Medical, New York, pp 147–148 321, 367, 376

24. Ferré S, Lluís C, Justinova Z, Quiroz C, Orru M, Navarro G, Canela EI, Franco R, Goldberg SR (2010) Adenosine-cannabinoid receptor interactions. Implications for striatal function. Br J Pharmacol 160(3):443–453

25. Taylor SB, Lewis CR, Olive MF (2013) The neurocircuitry of illicit psychostimulant addiction: acute and chronic effects in humans. Subst Abus Rehabil 4:29–43

26. Yager LM, Garcia AF, Wunsch AM, Ferguson SM (2015) The ins and outs of the striatum: role in drug addiction. Neuroscience 301:529–541

27. Walker FO (2007) Huntington's disease. Lancet 369(9557):218–228

28. Olsen CM (2011) Natural rewards, neuroplasticity, and non-drug addictions. Neuropharmacology 61(7):1109–1122

29. McDonald ML, MacMullen C, Liu DJ, Leal SM, Davis RL (2012) Genetic association of cyclic AMP signaling genes with bipolar disorder. Transl Psychiatry 2(10):e169

30. Santini E, Huynh TN, MacAskil A, Carter A (2013) Exaggerated translation causes synaptic and behavioural aberrations associated with autism. Nature 493:411–415

31. Everitt BJ, Robbins TW (2013) From the ventral to the dorsal striatum: devolving views of their roles in drug addiction. Neuroscience & Biobehavioral Reviews. Honoring Ann Kelley 37(9, Part A):1946–1954

32. Adedara IA, Rosemberg DB, Souza DO, Kamdem JP, Farombi EO, Aschner M, Rocha JBT (2015) Biochemical and behavioral deficits in lobster cockroach Nauphoeta cinerea model of methylmercury exposure. Toxicol Res 4:442–451

33. Adedara IA, Ego VC, Subair IT, Oyediran O, Farombi EO (2017) Quercetin improves neurobehavioral performance through restoration of brain antioxidant status and acetylcholinesterase activity in manganese-treated rats. Neurochem Res 42:1219–1229

34. Bradford MM (1976) Rapid and sensitive method for the quantitation of microgram quantities of protein utilizing the principle of protein-dye binding. Anal Biochem 72:248–254

35. Ellman GL, Courtney KD, Andres V Jr, Feather-Stone RM (1961) A new and rapid colorimetric determination of acetylcholinesterase activity. Biochem Pharmacol 7:88–95

36. Misra HP, Fridovich I (1972) The role of superoxide anion in the auto-oxidation of epinephrine and a simple assay for superoxide dismutase. J Biol Chem 247:3170–3175

37. Clairborne A (1995) Catalase activity. In: A.R. Greewald (ed) Handbook of methods for oxygen radical research. CRC Press, Boca Raton, pp. 2:37–242

38. Habig WH, Pabst MJ, Jakoby WB (1974) Glutathione S-transferases. The first enzymatic step in mercapturic acid formation. J Biol Chem 249:7130–7139

39. Rotruck JT, Pope AL, Ganther HE, Swanson AB, Hafeman DG, Hoekstra WG (1973) Selenium: biochemical role as a component of glutathione peroxidase. Science 179:588–590

40. Beutler E, Duron O, Kelly BM (1963) Improved method for the determination of blood glutathione. J Lab Clin Med 61:882–888

41. Wolff SP (1994) Ferrous ion oxidation in the presence of ferric ion indicator xylenol orange for measurement of hydroperoxides. Methods Enzymol 233:182–189

42. Farombi EO, Tahnteng JG, Agboola AO, Nwankwo JO, Emerole GO (2000) Chemoprevention of 2-acetylaminofluorene-induced hepatotoxicity and lipid peroxidation in rats by kolaviron-a Garcinia kola seed extract. Food Chem Toxicol 38:535–541

43. Bancroft JD, Gamble M (2008) Theory and practice of histology techniques, 6th edn. Churchill Livingstone Elsevier, London, pp 83–134

44. Erikson KM, Dorman DC, Lash LH, Aschner M (2007) Manganese inhalation by rhesus monkeys is associated with brain regional changes in biomarkers of neurotoxicity. Toxicol Sci 97:459–466

45. Bharti VK, Srivastava RS, Anand AK, Kusum K (2012) Buffalo (Bubalus bubalis) epiphyseal proteins give protection from arsenic and fluoride-induced adverse changes in acetylcholinesterase activity in rats. J Biochem Mol Toxicol 26:10–15

46. Akinrinade ID, Memudu AE, Ogundele OM (2015) Fluoride and aluminium disturb neuronal morphology, transport functions, cholinesterase, lysosomal and cell cycle activities. Pathophysiology 22:105–115

47. Ballard CG, Greig NH, Guillozet-Bongaarts AL, Enz A, Darvesh S (2005) Cholinesterases: roles in the brain during health and disease. Curr Alzheimer Res 2:307–318

48. Richetti SK, Rosemberg DB, Ventura-Lima J, Monserrat JM, Bogo MR, Bonan CD (2011) Acetylcholinesterase activity and antioxidant capacity of zebrafish brain is altered by heavy metal exposure. NeuroToxicology 32:116–122

49. Lebda MA, El-Neweshy MS, El-Sayed YS (2012) Neurohepatic toxicity of subacute manganese chloride exposure and potential chemoprotective effects of lycopene. Neurotoxicology 33:98–104

50. Chtourou Y, Fetoui H, Garoui EM, Zeghal N (2012) Improvement of cerebellum redox states and cholinergic functions contribute to the beneficial effects of silymarin against manganese induced neurotoxicity. Neurochem Res 37:469–479

51. Frei B (1994) Reactive oxygen species and antioxidant vitamins: mechanisms of action. Am J Med 97:5–13

52. Hawkins CL, Davies MJ (2001) Generation and propagation of radical reactions on proteins. Biochim Biophys Acta 1504:196–219

53. Sehgal A, Kumar M, Jain M, Dhawan D (2012) Synergistic effects of piperine and curcumin in modulating benzo (a) pyrene induced redox imbalance in mice lungs. Toxicol Mech Methods 22:74–80

54. Bickers DR, Athar M (2006) Oxidative stress in the pathogenesis of skin disease. J Invest Dermatol 126:2565–2575

55. Leipnitz G, Seminotti B, Fernandes CG, Amaral AU, Beskow AP, da Silva LB, Zanatta A, Ribeiro CA, Vargas CR, Wajner M (2009) Striatum is more vulnerable to oxidative damage induced by the metabolites accumulating in 3-hydroxy-3-methylglutaryl-CoA lyase deficiency as compared to liver. Int J Dev Neurosci 27(4):351–356

56. Kawanishi S, Yamamoto K (1991) Mechanism of site-specific DNA damage induced by methylhydrazines in the presence of copper (II) or manganese (III). Biochemistry 30:3069–3075

57. Surget S, Khoury MP, Bourdon JC (2013) Uncovering the role of p53 splice variants in human malignancy: a clinical perspective. Onco Targets Ther 7:57–68

58. Weng C, Li Y, Xu D, Shi Y, Tang H (2005) Specific cleavage of Mcl-1 by caspase-3 in tumor necrosis factor-related apoptosis-inducing ligand (TRAIL)-induced apoptosis in Jurkat leukemia T cells. J Biol Chem 280(11):10491–10500

59. Salvesen GS (2002) Caspases: opening the boxes and interpreting the arrows. Cell Death Differ 9(1):3–5

60. Hardwick JM, Soane L (2013) Multiple functions of BCL-2 family proteins. Cold Spring Harb Perspect Biol 5(2):a008722

61. Basu A, Haldar S (1998) The relationship between Bcl-2, Bax an p53: consequences for cell cycle progression and cell death. Mol Hum Reprod 4(12):1099–1109